Applied Computer Science 2025, vol. 21, no. 3, pp. 198–209
https://doi.org/10.35784/acs_8041

Submitted: 2025-07-04 | Revised: 2025-08-20 | Accepted: 2025-08-27

Keywords: microphone array, noise source, nitrogen generation, frequency

Grzegorz Barański [1*]
[1] Department Lublin University of Technology, Poland, g.baranski@pollub.pl
[*] Corresponding author: g.baranski@pollub.pl

Noise source analysis of the nitrogen generation system

Abstract

This study presents a comprehensive noise source analysis of a nitrogen generation system installed in an industrial production facility. The primary objective of the investigation was to determine the location of the dominant noise sources and to identify their respective sound pressure levels and frequency characteristics under operating conditions. Detailed measurements were made using a 16-microphone array combined with CAE Noise Inspector software for accurate sound field visualization and analysis. Experimental tests were conducted at three different locations within the system: the nitrogen generation unit (location 1), the nitrogen storage tank (location 2), and the exhaust pipe (location 3), with the latter further subdivided into three specific measurement points (3a, 3b, 3c) to account for variations along the length of the pipe. Each acoustic measurement session lasted three seconds, with data recorded at a high recording frequency of 204,800 Hz to ensure precise resolution across the frequency spectrum. The operating cycle of the nitrogen generator was divided into two main phases: phase 1, characterized by the transient sounds associated with valve actuation, and phase 2, dominated by the continuous sounds generated during nitrogen transfer to the storage tanks and exhaust. Recordings at site 1 captured both operational phases, while measurements at sites 2 and 3 focused exclusively on phase 2 in order to isolate relevant noise sources. The results provide a detailed and quantitative characterization of the acoustic emissions associated with the nitrogen generation process, providing valuable insights that can be used to develop targeted noise reduction strategies and contribute to future optimization of the system's mechanical design and operational efficiency.

1. INTRODUCTION

Sound source analysis is a widely used measurement technique. It is particularly important when it is necessary to identify the sound source, its amplitude and frequency. To measure all these parameters, microphone arrays are used. With these devices, equipped with several or a dozen directional microphones, it is possible to identify all the parameters mentioned above. The basic principles of this type of measurement are presented in (Baldinelli et al., 2021), where the authors introduce an innovative beamforming technique to improve the detection of distances and relative positions between noise sources in multi-source industrial environments. The method combines stereoscopic measurements and image processing to retrieve geometric information, including the distance between noise sources and their distance from the observer. This approach enhances standard beamforming by adding spatial context to noise mapping, although it suffers some loss of precision in highly reflective acoustic environments. Similar analyses can be applied, for example, to sound sources that are considered harmful due to excessive intensity or frequency levels that may be harmful to the human ear. In almost every industry, the human body is exposed to hazardous noise.

This problem is particularly relevant for large urban areas and airports. The paper (Zamponi et al., 2025) presents an experimental investigation of the acoustic and aerodynamic performance of flow-permeable fairings installed on a full-scale landing gear. The study shows that high-resistivity porous materials - such as fine wire meshes and diamond lattice structures - can reduce radiated noise by up to 16 dB in critical frequency ranges without the aerodynamic penalties associated with solid fairings. These results provide valuable insights for the development of low-noise technologies applicable to other systems.

Another hazardous area in urban agglomerations is congested roads. In their publication (Zhang & Wei, 2018), the authors presented the experimental identification of noise sources on a Volkswagen 2VQS EFI engine using an acoustic array and beamforming. The study shows that the generator side, intake side, and exhaust side each have distinct dominant noise sources, with the generator, cylinder block, and gear train identified as major contributors in the 1,000-2,000 Hz frequency range. The experiments also show that noise intensity increases with engine speed up to 2,500 rpm, after which changes are minimal. Locating the sources of noise may be useful in further work to reduce its level.

It should also be emphasized that vibrations caused by the operation of internal combustion engines can generate uncontrolled sound sources. In the publication (Caban et al., 2020), the authors used the effect of vibrations excited by the suspension of diesel engines for energy harvesting purposes, but such vibrations can also be detrimental to the strength of the structure.

The prediction of damage to mechanical components in terms of excessive wear is also discussed in the literature (Jonak & Krukow, 2017) and (Banas & Wilde, 2014). Both publications deal with the diagnosis of machine components by means of vibration analysis, which can of course be supplemented by acoustic analysis.

The human body is also exposed to hazardous noise sources in power plants. In an article (Fiebig, 2007), the author discusses noise generation mechanisms and noise reduction techniques in fluid power units and identifies the major noise sources using the sound intensity method. The study shows that components with larger sound radiating surfaces, such as the electric motor and oil reservoir, contribute significantly to the total noise radiated. Effective noise reduction requires addressing the loudest noise sources, which can be accomplished through methods such as reducing structure-borne sound transmission and using acoustic absorption materials within the tank.

Another example of excessive sound intensity is heavy equipment, such as that used on construction sites. The authors of the publication (Li et al., 2013) have investigated noise source detection on a tandem vibratory roller using surface noise intensity measurements and spectrum analysis. The study shows that the primary noise source is concentrated in the engine area, with engine combustion noise and exhaust fan noise being the main contributors. In addition, the analysis identifies cab floor noise leakage and characterizes the frequency of various engine components, providing a basis for noise control strategies.

Another example presented in the article (Bortnowski et al., 2020) relates directly to the use of an acoustic camera to verify the design and operation of belt conveyors by generating sound pressure level maps. The study identifies noise sources such as the electric motor, idler bearing, and belt misalignment at the tail pulley, and uses frequency analysis to locate abnormal operating noises. The research demonstrates the effectiveness of the acoustic camera in locating and analyzing belt conveyor noise.

There are also more detailed studies, conducted on a larger scale, which, in addition to the acoustic analysis of industrial equipment, examine the impact of noise not only on a specific production facility, but also on its surroundings. This approach is presented in an article (Fiebig, 2019), which outlines a methodology for identifying and reducing noise in an industrial plant using an acoustic camera with beamforming to locate the main noise sources. The study includes noise level measurements, noise mapping using 3D modeling, and the implementation of noise reduction measures, ultimately demonstrating that the proposed approach can effectively reduce noise levels to acceptable levels in nearby residential areas.

The available literature also includes cases of sound analysis to identify damage to machinery and equipment. The article (Pavlikova et al., 2018) discusses the use of an acoustic camera to identify failures in machinery and equipment, with a specific focus on a four-wheel lawn mower. The study shows that analyzing noise sources with an acoustic camera can effectively locate failures, which can help implement targeted maintenance and reduce downtime. This method offers a promising approach for early diagnosis and improved maintenance strategies in industrial environments.

It is well known that rotating or moving elements can also generate sound. The above mentioned measurement method is also used to analyze this type of phenomenon. In the publication (Nashimoto et al., 2008), the authors investigate the aerodynamic noise source distribution around a rotating fan blade by measuring the noise signal and visualizing the velocity field. The study uses microphone arrays and phase-averaged PIV to measure local noise levels and flow fields, and then uses cross-correlation analysis to associate noise signals with velocity fluctuations. The results indicate that noise sources are located near the leading and trailing edges of the rotating fan blade and are influenced by flow separation, reattachment, tip vortices, and vortex shedding.

Similar research was conducted for an autogyro model and presented in an article (Magryta et al., 2017), where an acoustic camera was used to analyze the noise distribution, focusing on the location of noise sources in an autogyro model. In this study, a 16-microphone acoustic camera with Noise Inspector software was used to obtain acoustic maps and sound power levels during rotor prerotation and main engine operation. The results identified the main noise source as the propeller, demonstrating the effectiveness of acoustic cameras in visualizing and measuring sound intensity in aircraft noise analysis.

Similar studies are also being conducted to locate aerodynamic noise sources. As presented in the paper (Ershov et al., 2020), which investigated a new beam microphone array that allows rapid repositioning of the microphones in radial and angular coordinates. The performance of the array was validated by localizing aerodynamic noise sources from a turbulent jet, with results compared to a commercial Bruel & Kjaer array, demonstrating comparable accuracy in source location and level measurements.

Noise issues affect not only small devices, but also large areas. For example, one article (Fredianelli et al., 2021) analyzes the complexity of noise emissions in port environments and proposes a structured classification system to improve the accuracy of noise mapping. It identifies five main categories of noise sources - road, rail, ship, port and industrial - and proposes further subdivisions to facilitate the assignment of responsibility and planning of mitigation measures. The study, supported by the INTERREG Maritime Programme, highlights the need for standardized methodologies to address regulatory gaps and improve citizen protection in urban areas adjacent to ports.

The use of microphone arrays allows accurate analysis of noise maps over larger areas, as presented in the publication (Licitra et al., 2022). The article presents new visualization tools for strategic noise maps designed to improve the understanding and communication of environmental noise data. These maps use polygons and colors to show the predominant noise source at each point, and I-NSP maps additionally incorporate noise exposure levels. Application of these maps in port areas demonstrates their potential to assist in assigning responsibility for noise exceedances and in locating acoustic monitoring stations.

Using the appropriate equipment configuration, the source can also be identified at great distances. The article (Bocanegra et al., 2022) examines the use of acoustic cameras to characterize noise in a port, addressing the challenges associated with multiple simultaneous noise sources and the difficulties of using traditional measurement techniques in a port environment. The study identifies various noise sources in the Port of Genoa and proposes a methodological framework for the use of acoustic cameras in port noise studies, highlighting their potential as valuable tools for port noise monitoring and management.

All these examples confirm that the use of a microphone array for sound recording and localization is justified. In the presented article, the author used the same method to analyze the sound source of the nitrogen production equipment in the KOSTAL INDUSTRIE ELEKTRIK POLAND Sp. z o.o. plant. The aim of the research was to determine the noise level and frequency of the sounds in order to obtain the information necessary to modify the workplace in order to make it quieter. Tests were conducted in three different microphone array configurations representing the nitrogen generator, nitrogen tank, and exhaust pipe, with three separate array settings representing three different sections of the exhaust pipe.

2. MEASUREMENT DESCRIPTION

The equipment used to produce nitrogen for a PCB production line. The Atlas Copco NGP300+ system is a dedicated unit. This nitrogen generator complies with the ISO Grade Designs: ISO 8 standard and produces high purity, high flow nitrogen up to 99.999%. It is used in industries such as pharmaceuticals, semiconductor manufacturing, food and beverage (storage and packaging), chemicals, metal heat treatment, plastic injection molding, electronics, laser cutting, cable and fiber optics, and glass. The unit monitors the quality of supply air and gas output 24/7, protecting N2 applications and products and eliminating energy waste during low demand and colder temperatures for up to 40% energy savings (Terra Universal, (n.d.).

The unit has been installed at the KOSTAL INDUSTRIE ELEKTRIK POLAND Sp. z o.o. The purpose of the measurements was to determine the location of the sound source of the above mentioned equipment and to identify its intensity and frequency. The tests were performed using a microphone array (16 microphones) and the CAE Noise Inspector program. This advanced instrumentation facilitates the conversion of acoustic signals into visual representations - such as still images or dynamic video frames - allowing precise and immediate detection of noise sources within the measurement environment. The system enables real-time identification of the acoustic source and quantification of the emitted sound pressure level. Compared to conventional measurement techniques, this approach significantly reduces the time required for data acquisition and analysis (Wibroakustyka, n.d.). The measurement apparatus consists of a planar microphone array consisting of 16 individual sensors symmetrically arranged around a centrally positioned high-definition camera. The system also includes dedicated acoustic and visual signal processing modules, all integrated and controlled by a portable computer.

The Noise Inspector system incorporates the following key components (Magryta et al., 2017):

- planar array of microphones,
- Microsoft LifeCam Studio 1080p HD optical sensor,
- 16 G.R.A.S. 40PH uniaxial measurement microphones,
- PXIe-1073 ICP signal acquisition interface (National Instruments),
- PXI-4496 data acquisition card,
- mobile computing platform,
- CAE Noise Inspector software, version 6.0.

A view of the microphone array with accessories is shown in Fig. 1.

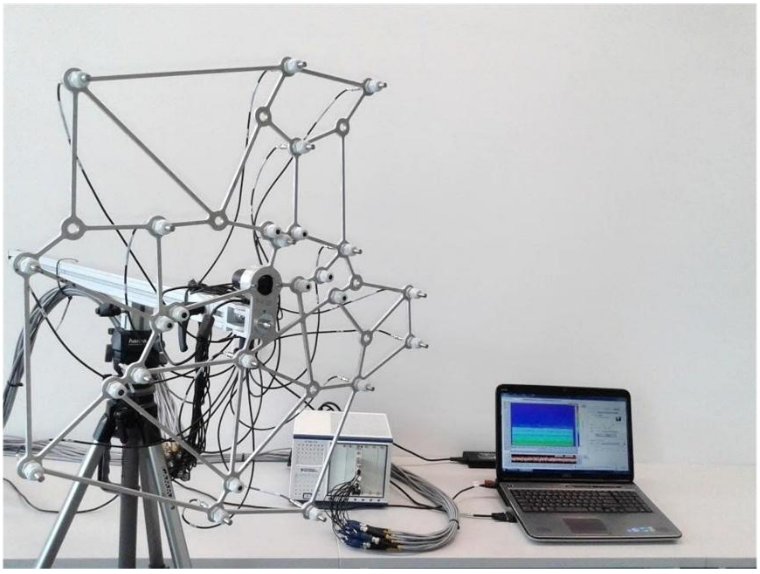

Fig. 1. View of the microphone array with accessories (Magryta et al., 2017)

This methodology offers several advantages that increase both efficiency and measurement fidelity. The modular structure of the system allows it to be tailored to specific experimental requirements. The main advantages of this approach include the following (Magryta et al., 2017):

- single-measurement capability with no need for repeated recordings,
- improved accuracy relative to traditional measurement microphones,
- non-intrusive data acquisition enabling measurements during normal operation of machinery or systems,
- ability to generate detailed acoustic maps for identifying dominant noise sources,
- capacity to isolate specific components responsible for noise generation,
- elimination of the need to interrupt operational processes at the measurement site,
- effective performance in acoustically complex and reverberant environments,
- applicability to both indoor laboratory conditions and open-field environments.

The basic principle of the acoustic camera system is based on the spatial detection of acoustic energy at different pressure levels. A characteristic feature of the system is the ability to refocus after data processing, which allows the generation of multiple acoustic images from a single data set without the need to repeat measurements. In addition, the system offers a live preview function that allows real-time visualization and preliminary analysis of measurement data (Vibroacoustics, 2025). Figure 2 shows a view of the CAE Noise Inspector program with a detailed window description.

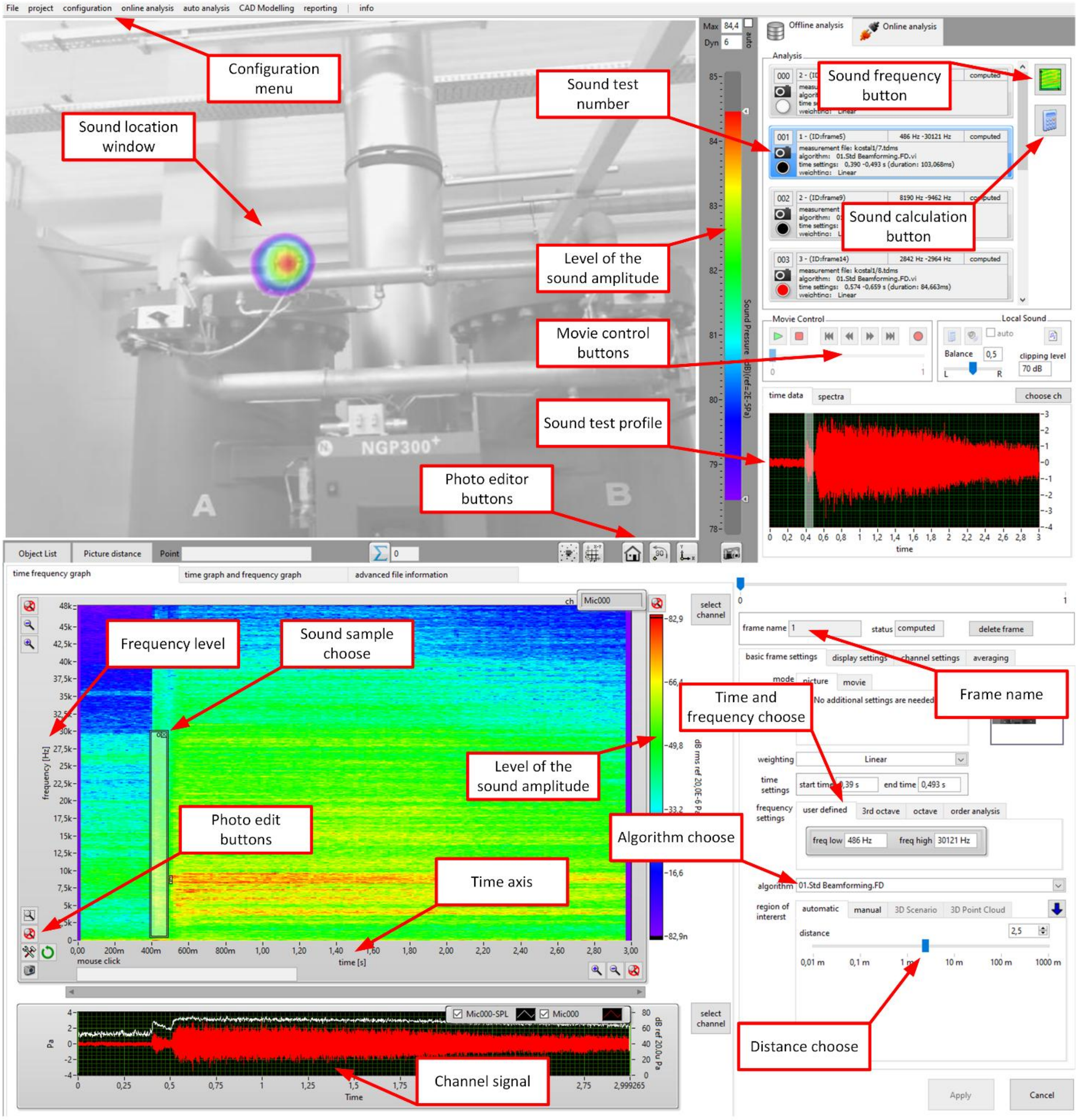

Fig. 2. View of the CAE Noise Inspector program, with detailed windows description

Tests were conducted in three different microphone array configurations, as shown in Figure 3 and Figure 4:

- location 1 representing the nitrogen generation installation,
- location 2 representing the nitrogen tank,
- location 3 represents the exhaust gas pipe, for which three separate array settings were made, representing three different sections of the ejection tube (3a, 3b, 3c).

The object was located in a large production hall with constant environmental conditions. Environmental data was recorded during the tests:

- the temperature was 23 °C,
- the relative humidity was 52 %,
- the background noise was approx. 40 dB.

Each measurement lasted 3 seconds, and the sound recording frequency was 204,800 Hz. The GRAS 40PH-10 CCP microforms used were characterized by:

– Frequency range: 10 Hz to 20,000 Hz,
– Dynamic range: 33 dB to 135 dB,
– Set sensitivity at 250 Hz (±2 dB): 50 mV/Pa.

The nitrogen generator worked in two stages. In the first stage (Phase 1), the sound of the valves opening was audible, and in the second stage (Phase 2), the sound of the nitrogen being transferred to the tanks and the sound of the exhaust gases being expelled through the exhaust pipe was audible (Fig. 5). For site 1, the first and second stages were recorded, while for sites 2 and 3, only the second stage was recorded.

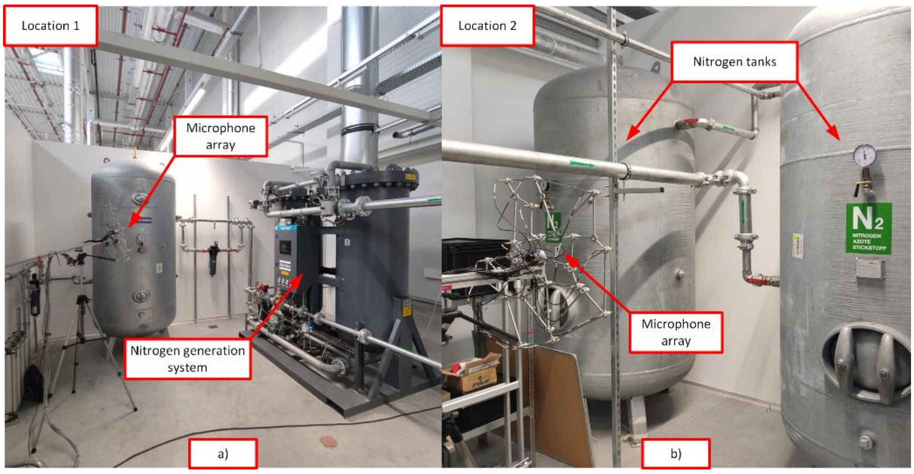

Fig. 3. The first two microphone array settings - a) location 1, b) location 2

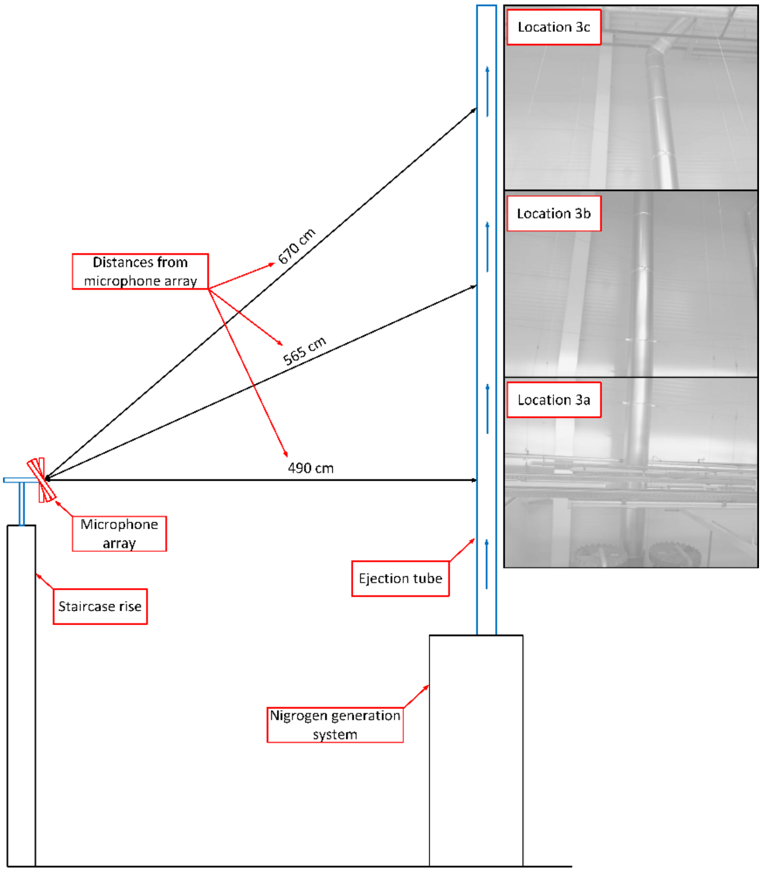

Fig. 4. Third microphone array setting (locations 3a, 3b, and 3c)

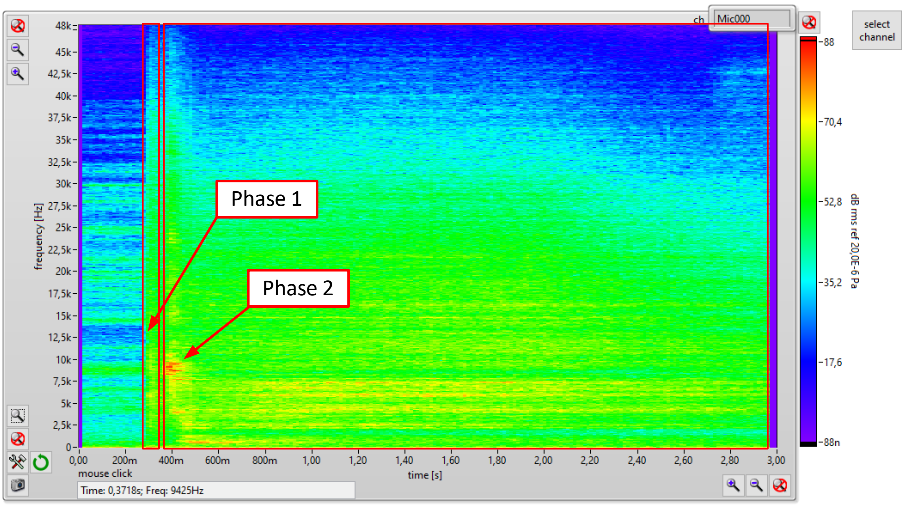

Fig. 5. Two time phases (phase 1 and phase 2)

3. RESULTS AND DISCUSSION

The results of the sound recordings were analyzed using a special software for processing microphone arrays. The program allowed the identification of the sound source for a specific frequency range and time of occurrence. In order to analyze the phenomena occurring in both phases of the device's operation, the results were analyzed, from which three cases were identified for site 1 and one case for site 2. The whole is presented in (Fig. 6, 7, 8, 9), where the following are specified:

– Fig. 6 sound of valve opening, frequency range 486 – 30,121 Hz,
– Fig. 7 sound of nitrogen transfer through a pipe connection, frequency range 8,000 – 9,895 Hz,
– Fig. 8 horn sound of exhaust gas discharge, frequency range 2,842 – 2,964 Hz,
– Fig. 9 horn sound of nitrogen transfer to tanks, frequency range 4,178 – 4,251 Hz.

In all of the variants presented, increased sound intensity is visible in the equipment components that were in operation at the time. All recorded sounds had an amplitude level above 85 dB. The highest amplitude was recorded for phase 2, which was over 91 dB in the case of nitrogen transmission through a pipe connection. The acoustic image shown in Figure 6 clearly indicates that the sound source is located directly at the valve, confirming the high accuracy of the method. In this case, the sound intensity is concentrated in a single, distinct point, suggesting a point source rather than a diffuse emission source.

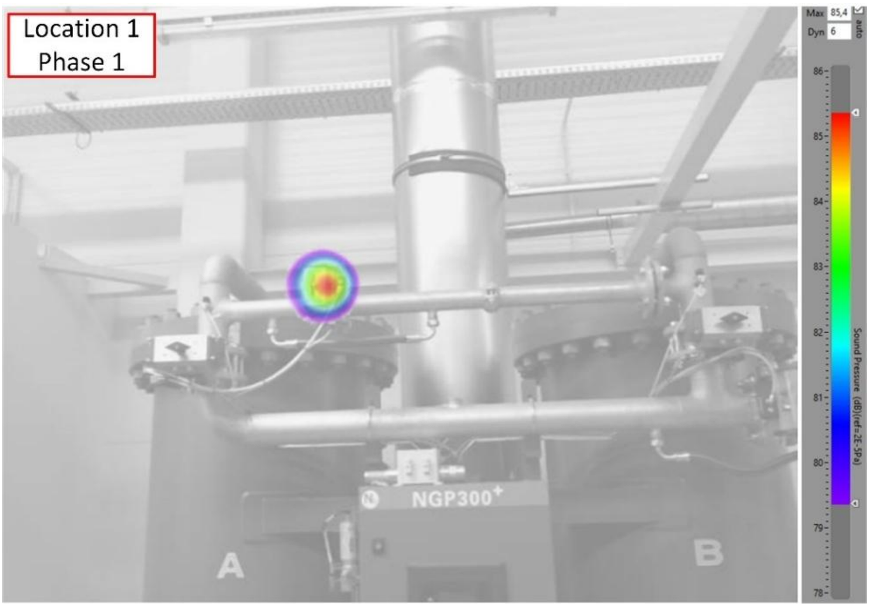

Fig. 6. Identifying the sound source in location 1, sound of valve opening, frequency range 486 – 30,121 Hz

Figure 7 shows nitrogen flowing through a pipe joint. The recording captured sound in the frequency range of 8,000 to 9,895 Hz. The acoustic image shows that the sound source is distributed along a section of the pipe, consistent with the flow of the medium through the pipe.

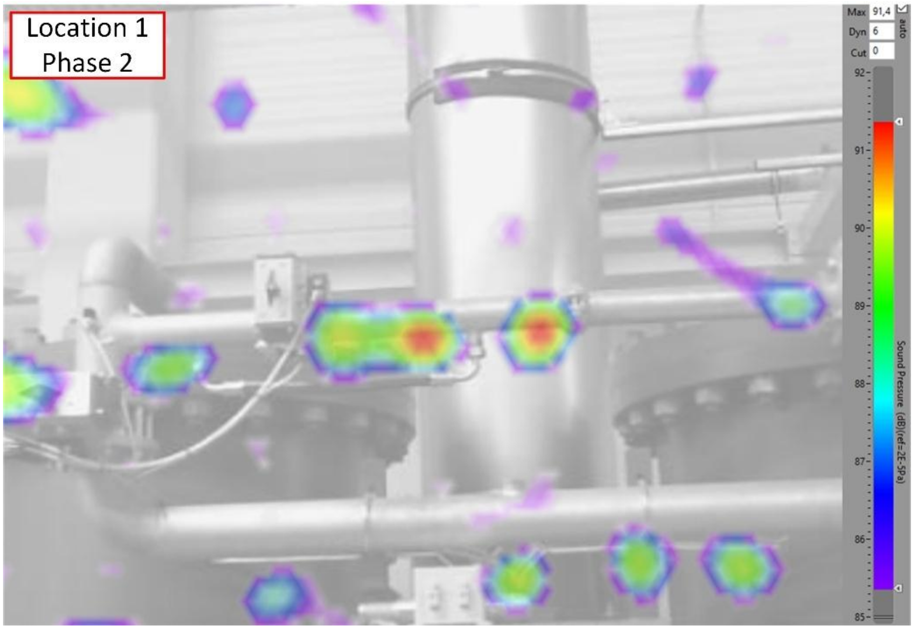

Fig. 7. Identifying the sound source in location 1, sound of nitrogen transfer through a pipe connection, frequency range 8,000 – 9,895 Hz

The sound during exhaust emission is shown in Fig. 8. This case is characterized by a narrower frequency band, from 2,842 to 2,964 Hz. The sound source is also localized, but it is visible as a larger, diffuse area covering several components of the device. This may indicate that the sound is propagating to adjacent components in addition to the main source.

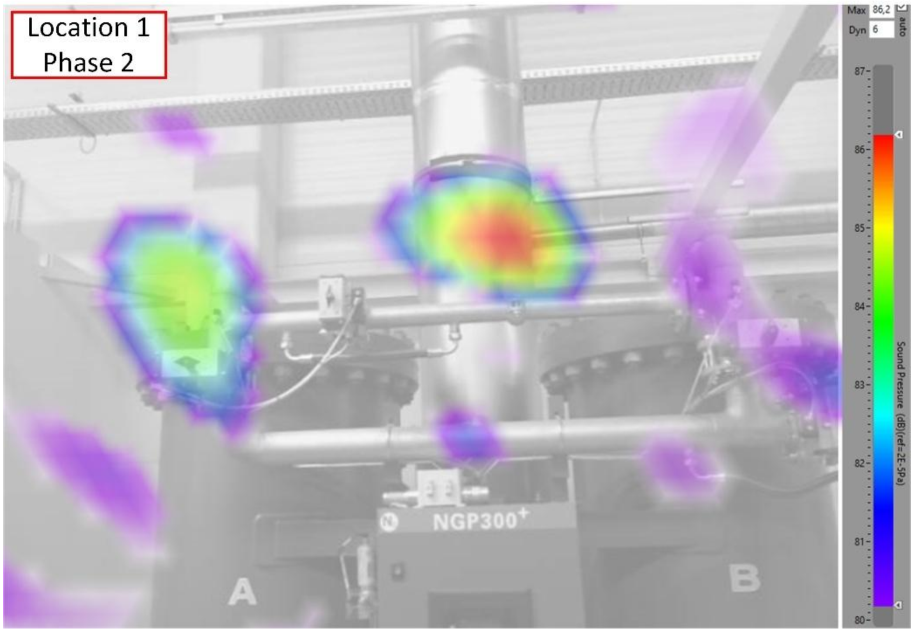

Fig. 8. Identifying the sound source in location 1, horn sound of exhaust gas discharge, frequency range 2,842 – 2,964 Hz

During the nitrogen transfer phase to the tank, a sound with a frequency between 4,178 and 4,251 Hz was identified (Fig. 9). As in the previous cases, the software indicated an increased sound intensity in the area of the components operating at that time.

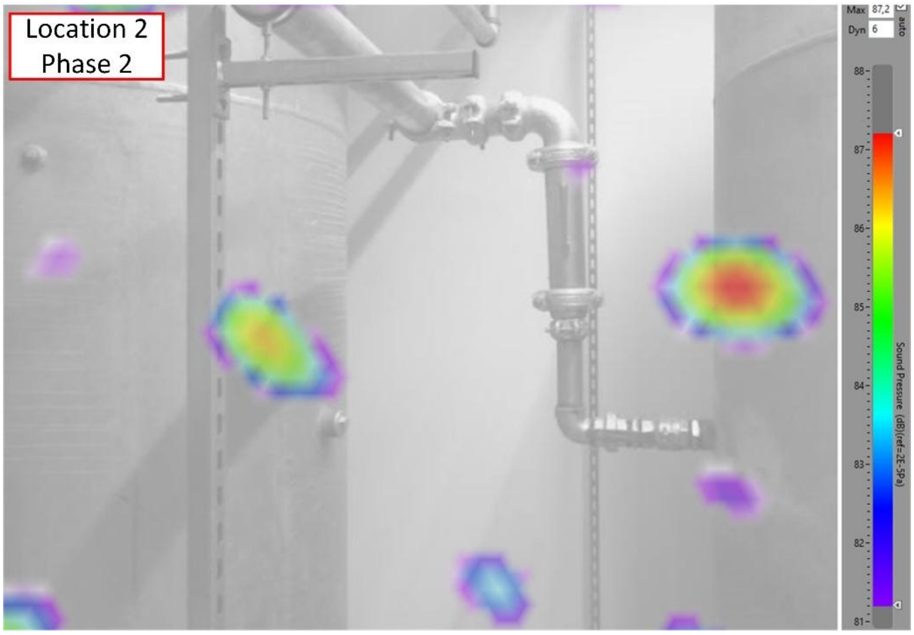

Fig. 9. Identifying the sound source in location 2, horn sound of nitrogen transfer to tanks, frequency range 4,178 – 4,251 Hz

For a more detailed analysis of the frequency range in (Fig. 6), two graphs showing the relationship between amplitude and sound frequency are presented for two selected recordings:

- Fig. 10a location 1 phase 2 sound of nitrogen transfer through a pipe connection, increase in amplitude for the frequency range 8,000 – 9,895 Hz, the recorded amplitude was over 91 dB, which is the highest value recorded in the entire study,
- Fig. 10b sound of nitrogen transfer to tanks, amplitude increase for the frequency range 4,178 – 4,251 Hz.

As can be seen in the figure, in both cases there is a significant increase in sound amplitude in certain frequency ranges. For the sample shown in the graph on the left, an increase in amplitude of 25 dB was observed, while for the test shown in the graph on the right, an increase in amplitude of 22 dB was observed.

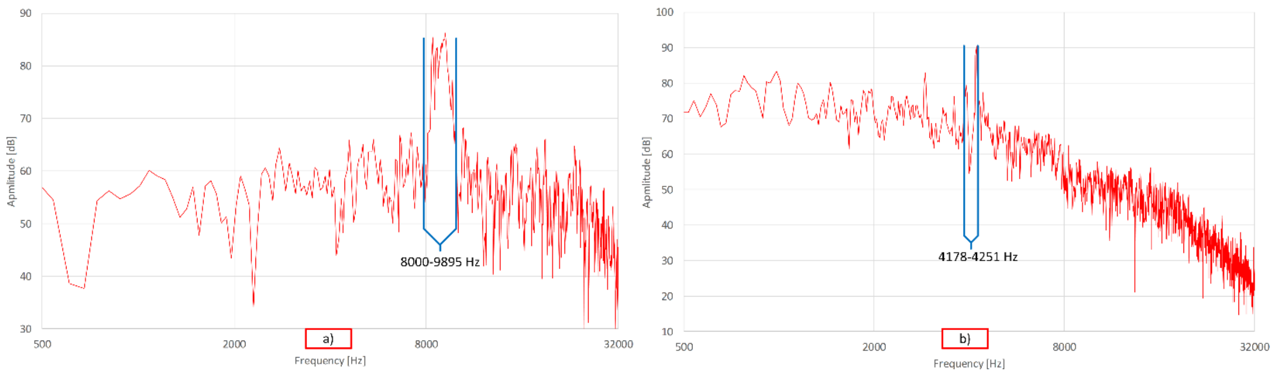

Fig. 10. Average sound intensity value as a function of frequency for two selected cases

The results for location 3 are presented similarly, with three separate measurements for each section of the ejection tube. To standardize the results, the same frequency range was selected for each section: 3,800 - 4,050 Hz. Figures 11, 12 and 13 show areas of higher sound amplitude. The initial gas ejection visible in Fig. 11 (location 3a) is identical to the first phase of gas ejection. However, in the following sections (location 3b - Fig. 12) and location 3c - Fig. 13), the exact source of the sound is not visible. The recorded signal appears to be scattered, and the sound of the gas ejection was reflected off the surrounding pipe infrastructure, making it impossible to pinpoint a specific area.

The initial gas discharge is visible as a clearly localized sound source with increased amplitude (Fig. 11). The view of the noise sources is similar to that recorded at the first location.

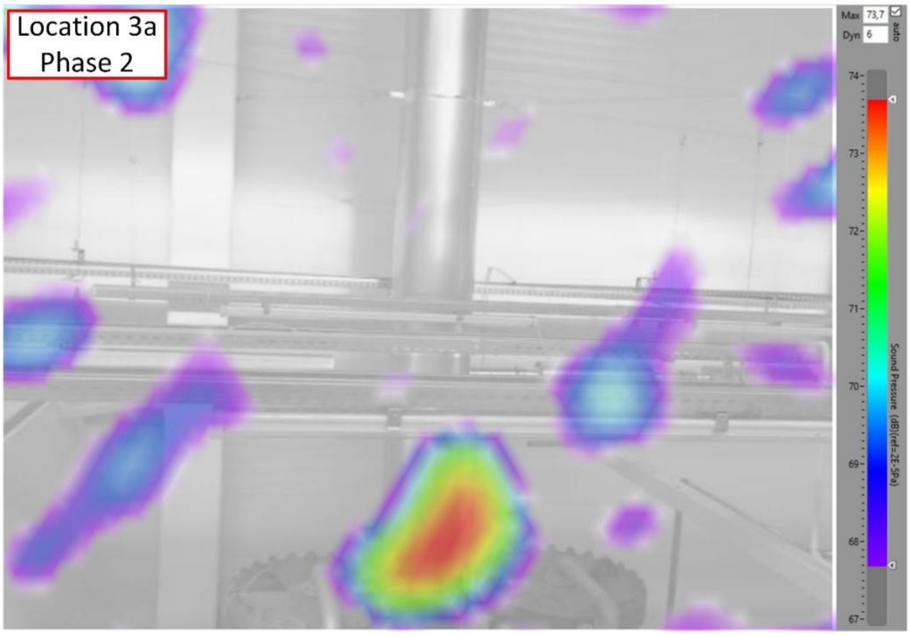

Fig. 11. Identification of the sound source in settings 3a (sound of exhaust gas ejection)

The acoustic images in Figures 12 and 13 show many scattered areas of increased amplitude, which is characteristic of the phenomenon of reflection and scattering of sound waves in a complex pipe environment. This may also be due to the fact that the microphone array was not placed perpendicular to the outlet pipe, which was long and hung high, limiting the ability to place the array perpendicular to the outlet channel and move it vertically a short distance to take multiple measurements perpendicular to the pipe along its entire length.

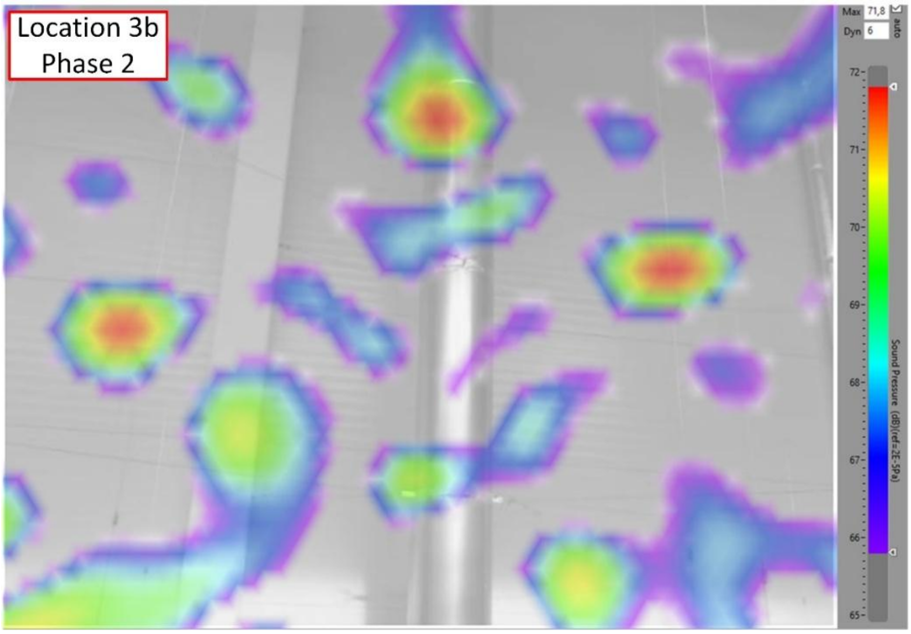

Fig. 12. Identification of the sound source in settings 3b (sound of exhaust gas ejection)

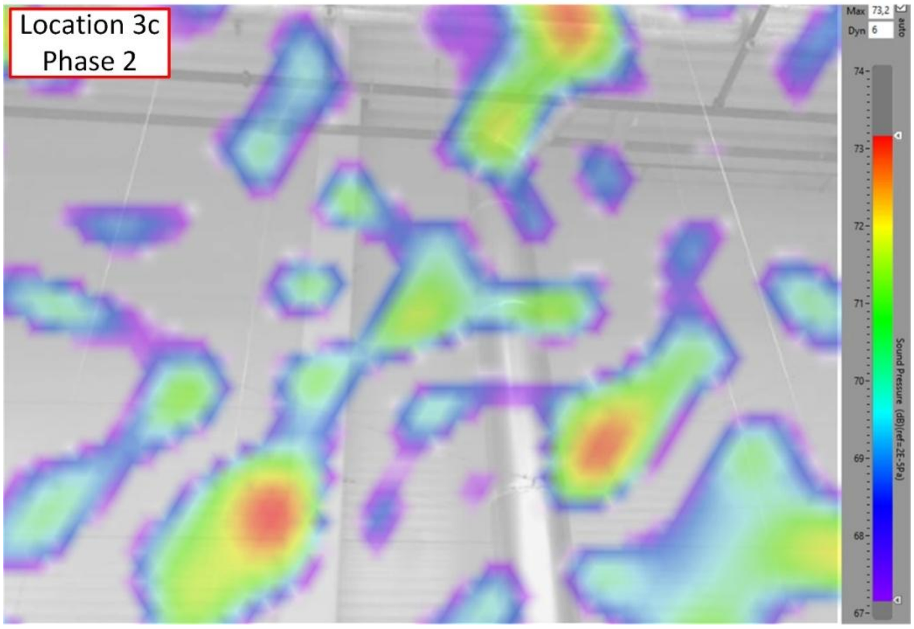

Fig. 13. Identification of the sound source in settings 3c (sound of exhaust gas ejection)

4. CONCLUSIONS

The analysis of sound recordings using a microphone array allowed the identification and characterization of various noise sources generated during the operation of a nitrogen generation device for a printed circuit board production line. Key findings include:

- Different sound sources and their frequency characteristics: Four main sound sources were identified (valve opening, nitrogen transfer through a pipe connection, exhaust gas discharge, nitrogen transfer to tanks), each with a specific frequency range. The widest range (486 - 30,121 Hz) was recorded for the valve opening sound.
- Increased sound intensity in active components: In all analyzed variants, a significant increase in sound intensity was observed in those components of the equipment that were active at a given moment. This confirms the effectiveness of the method in locating noise sources.
- High amplitude of the recorded sounds: All recorded sounds had an amplitude greater than 85 dB. A particularly high amplitude of more than 91 dB was recorded for the sound of nitrogen transmission through the tube connection in phase 2 of the device's operation, indicating a potentially high noise level in this phase.
- A clear increase in amplitude in certain frequency ranges: A detailed analysis of the relationship between amplitude and frequency showed significant amplitude increases (of 25 dB and 22 dB) in certain frequency ranges for nitrogen transfer sounds. This suggests the presence of dominant frequency components for these phenomena.
- Challenges of sound source localization in complex environments: In the case of Site 3, despite the initial identification of gas emissions, the subsequent measurements (Sites 3b and 3c) did not allow for precise localization of the sound source. The scattered signal and reflections from the surrounding infrastructure made accurate localization difficult, highlighting the challenges of acoustic analysis in environments with complex infrastructure.
- Acoustic insulation of the exhaust pipe and pipe connections could reduce the high amplitude noise (> 90 dB) observed during Phase 2 operations.
- Design modifications to the valve actuation system, such as the use of low-noise or pneumatically damped valves, could reduce the transient noise peaks detected in the 486 - 30,121 Hz range.
- The use of silencers or resonators tuned to the dominant frequency bands (e.g. 8,000 - 10,000 Hz) could significantly reduce tonal noise.

– Optimization of the tube geometry or the introduction of acoustic baffles at certain sections could help to eliminate the sound reflections observed in the ejection tube, thus improving both noise levels and measurement accuracy in complex installations.
– Future work could also include numerical modeling of acoustic wave propagation in the system to evaluate the effectiveness of proposed modifications prior to physical implementation.

These conclusions provide a valuable basis for further research to reduce the noise generated by the device and optimize its operation in terms of acoustics, and demonstrate the possibilities and difficulties involved in performing this type of measurement.

Acknowledgments

The project/research was financed in the framework of the Lublin University of Technology funds conducting scientific activities FD - discipline fund, funded by the Polish Ministry of Science and Higher Education - Article 365 (2) of July 20, 2018.

REFERENCES

Baldinelli, G., Bianchi, F., Costarelli, D., D'Alessandro, F., Scrucca, F., Seracini, M., & Vinti, G. (2021). Innovative techniques for the improvement of industrial noise sources identification by beamforming. *Noise Mapping*, *8*(1), 129–137. https://doi.org/10.1515/noise-2021-0010

Banas, A., & Wilde, K. (2014). Vibration diagnostics of footbridge with use of rotation sensor. *Applied Computer Science*, *10*(4), 38–49.

Bocanegra, J.A., Borelli, D., Gaggero, T., Rizzuto, E., & Schenone, C. (2022). A novel approach to port noise characterisation using an acoustic camera. *Science of the Total Environment*, *808*, 151903. http://dx.doi.org/10.1016/j.scitotenv.2021.151903

Bortnowski, P., Nowak-Szpak, A., Ozdoba, M., & Krol, R. (2020). The acoustic camera as a tool to identify belt conveyor noises.

Caban, J., Litak, G., Ambrożkiewicz, B., Gardyński, L., Stączek, P., & Wolszczak, P. (2020). Impact-based piezoelectric energy harvesting system excited from diesel engine suspension. *Applied Computer Science*, *16*(3), 16-29. https://doi.org/10.23743/acs-2020-18

Ershov, V. V., Sorokin, E. V., Palchikovskiy V. V., & Korin, I.A. (2020). Study of new beam microphone array operation based on aerodynamic noise sources localization. *2020 International Conference on Dynamics and Vibroacoustics of Machines (DVM)* (pp. 1-7). IEEE. https://doi.org/10.1109/DVM49764.2020.9243905

Fiebig, W. (2007). Location of noise sources in fluid power machines. *International Journal of Occupational Safety and Ergonomics*, *13*(4), 441-450. https://doi.org/10.1080/10803548.2007.11105102

Fiebig, W. (2019). Use of acoustic camera for noise sources localization and noise reduction in the industrial plant. *Archives of Acoustics*, *45*(1), 111-117. https://doi.org/10.24425/aoa.2020.132487

Fredianelli, L., Bolognese, M., Fidecaro, F., & Licitra, G. (2021). Classification of noise sources for port area noise mapping. *Environments, 8*(2), 12. https://doi.org/10.3390/environments8020012

Jonak, K., & Krukow, P. (2017). Matching pursuit algorithm in assessing the state of rolling bearings. *Applied Computer Science*, *13*(2), 61-71. https://doi.org/10.23743/acs-2017-14
Journal of Sustainable Mining, *19*(4), 7. https://doi.org/10.46873/2300-3960.1036

Li, L., Feng, Z., & Zhao, L. (2013). Recognition of noise source on tandem vibratory roller. *Advanced Materials Research*, *694-697*, 439-443. https://doi.org/10.4028/www.scientific.net/AMR.694-697.439

Licitra, G., Bolognese, M., Chiari, C., Carpita, S., & Fredianelli, L. (2022). Noise source predominance map: A new representation for strategic noise maps. *Noise Mapping*. *9*(1), 269–279. https://doi.org/10.1515/noise-2022-0163

Magryta, P., Skiba, K., & Czyż, Z. (2017). Identification of noise generated by driving set of autogyro using an acoustic camera. *Advances in Science and Technology Research Journal*, *11*(4), 247–251. https://doi.org/10.12913/22998624/80825

Nashimoto, A., Fujisawa, N., Nakano, T., & Yoda, T. (2008). Visualization of aerodynamic noise source around a rotating fan blade. *Journal of Visualization*, *11*(4), 365-373. https://doi.org/10.1007/BF03182205

Pavlikova, L., Hricová, B., & Lumnitzer, E. (2018). Acoustic camera as a tool for identifying machinery and equipment failures. *Advances in Science and Technology Research Journal*, *12*(1), 322–328. https://doi.org/10.12913/22998624/87110

Terra Universal. (n.d.). *NGP300+ Technical specification*. https://www.terrauniversal.com/ngp300-on-site-psa-nitrogen-generator-atlas-copco.html

Wibroakustyka. (n.d.). *Acoustic camera noise Inspector for quick location of noise sources*. www.wibroakustyka.com.pl

Zamponi. R., Rubio Carpio, A., Avallone. F., & Ragni, D. (2025). Noise source analysis of porous fairings in a scaled landing gear model. *Aerospace Science and Technology*, *158*, 109885. https://doi.org/10.1016/j.ast.2024.109885

Zhang, C., & Wei, L. (2018). Experiment on noise source identification based on acoustic array. *IOP Conference Series: Earth and Environmental Science*, *208*, 012071. https://doi.org/10.1088/1755-1315/208/1/012071